

REFRACTORIES FOR THE GLASS INDUSTRY

UDC 666.1.031.224

BOTTOM BLOCK FOR GLASS FURNACES: FIRED OR CONCRETE?

V. P. Migal',¹ V. V. Skurikhin,^{1,2} A. P. Margishvili,¹ P. E. Alekseev,¹ and A. A. Kovalenko¹

Translated from *Steklo i Keramika*, No. 9, pp. 12 – 19, September, 2011.

Comparative studies of the properties of calcined fireclay articles and articles made of low-cement refractory concretes (LCRC), fired at different temperatures and non-fired, used for the masonry of the bottom structure of tank glass furnaces (bottom block) have been performed. Experimentally obtained data on the thermo-physical properties, CLTE, glass stability of articles made of LCRC and calcined fireclay articles are presented. It is shown that fired fireclay articles are desirable to increase the service life of the furnace.

Key words: glassmaking furnace, bottom block, fireclay articles, low-cement refractory concretes, thermal conductivity, thermal diffusivity, CLTE, glass attack resistance.

The bottom block in modern tank glassmaking furnaces no longer functions as a working lining in direct contact with molten glass. However, the remaining functions of the bottom block are no less important: structural — the main carrying structure (support) of the entire furnace; safeguarding — protective (reinforcing) lining; heat-engineering — heat insulation of the furnace bottom. Data obtained by design organizations show that the temperature on the “hot” surface of the bottom block can reach 1300 – 1400°C depending on the degree of wear of the bakor lining.

Conventionally, calcined fireclay and mullite articles are used for the bottom block. The manufacture of such articles has been mastered at the Borovichi Refractory Works [1]. In recent years, active advancement and application of concrete articles have begun and publications on their use for the bottom structure of glassmaking furnaces have appeared [2 – 6]. Concrete articles are much more practicable and less expensive to manufacture: vibrational molding does not require powerful presses, the press-fixture is weaker and inexpensive, the lack of firing and the associated shrinkage makes it possible to conserve fuel and obtain articles with minimal dimensional deviations.

To determine the advantages and drawbacks of non-fired concrete and fired articles, studies of each group of articles mentioned were performed at the Research Center for Improving Technology and Production at the Borovichi Refractory Works (BRW), JSC.

All articles made of low-cement refractory concretes (LCRC) belong to the same class of refractory materials and are of the same nature — a composition of refractory fill and a matrix consisting of high-alumina cement and disperse and reactive alumina [7 – 9], so that their physical properties and the character of the chemical interaction with silicate melts, including the main metallurgical slag and glass melts, are similar to one another. On this basis the present authors believe that the research results obtained for the production materials used at BRW can be extended to the materials used by other producers.

MATERIALS STUDIED

Samples of calcined fireclay articles of the sorts ShSU-33 and ShSU-40 (GOST 7151–74) from the operating process stream of the steel-pouring pit shop at BRW were studied [10]. Samples, made of low-cement refractory concrete (LCRC) of the sort Borcast-50 W (TU 14-194-271–05) with fireclay fill, in the form of 230 × 114 × 65 mm articles and cubes with edge length 70 mm were made according to the composition and method of production developed at BRW [7]. The physical-chemical and thermo-mechanical properties of the articles are close (Table 1).

METHODS OF STUDY

The thermal conductivity of the materials was determined according to GOST 12170–85 at average sample temperature 320, 450, and 630°C.

¹ Borovichi Refractory Works, Borovichi, Russia.

² E-mail: vskurihin@borovichi-nov.ru.

The linear thermal expansion coefficient (CLTE) was determined on a DIL 402C dilatometer manufactured by Netzsch. The samples consisted of $5 \times 5 \times 50$ mm blocks and cubes with edge length 50 mm.

The glass attack resistance was determined by the crucible method. Cubes with 70 mm edges were cut from calcined fireclay articles of sort ShSU-33 and ShSU-40; a diamond drill was used to drill a 36 mm in diameter, 30 mm deep opening in the samples. Openings in concrete samples were made during molding. A weighed amount of ground glass (1–0 mm fractions) with mass about 40 g was poured into the pocket of the crucible and the sample was calcined at temperature 1400°C with 5-h soaking. After the tests the samples were cut through the center of the pocket (in the vertical plane) and the degrees of permeation and corrosion were evaluated by analyzing digital images in the INCA Mapping program. Petrographic studies were performed on thin specimens with scanning optical (Nikon) and electron (JEOL-6380LV) microscopes as well as with an INCA energy dispersive spectrometer.

RESULTS AND DISCUSSION

The calcined fireclay articles taken from the process stream were not subjected to further processing. The articles made of Borcast-50 W LCRC were left standing, after molding completion, for 3 days under natural conditions, after which they were heat-treated at temperatures 200, 400, 600, 800, 1000, and 1300°C with soaking at the maximum temperature for 2 h.

Thermal Conductivity. The results of the thermal conductivity measurements performed on the experimental materials are presented in Fig. 1. The thermal conductivity of the calcined ShSU-33 and ShSU-40 articles increases with temperature. The temperature dependence of the thermal conductivity of the Borcast-50 W LCRC follows different directions and depends on the heat-treatment temperature of the articles; the lowest thermal conductivity is observed for

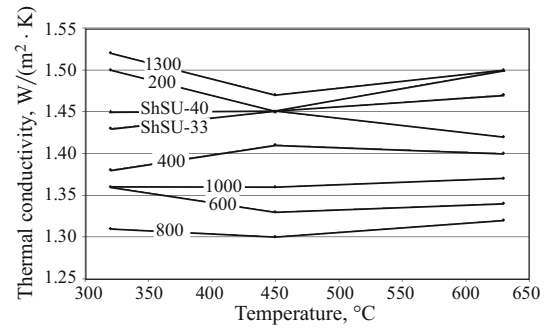
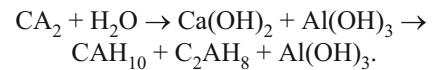
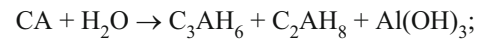


Fig. 1. Thermal conductivity of materials versus temperature (the numbers show the heat-treatment temperature of Borcast-50 W LCRC).

heat-treatment temperature 800°C. The change of the thermal conductivity is associated with a change in the structure of the concrete. During the initial period (after the articles are allowed to stand under natural conditions, when hydration of the minerals of high-alumina cement (HAC) occurs), the structure of the concrete is formed by bonds between hydrated HAC crystals, joined into stable three-dimensional structures, as well as by the adhesion properties of gel-like $\text{Al}(\text{OH})_3$, which is formed during the hydration of HAC. The hydration process can be described by the reactions



On heating the hydrate embryos lose water and break down, open porosity increases, and interparticle bonds weaken, resulting in lower thermal conductivity. Above 800°C the cement binding completely degrades; as reactive alumina and calcium aluminates in HAC (CA and CA_2) interact, calcium hexa-aluminate (CA_6) forms and sintering starts (the products of degradation have high activity). As CA_6 forms, the volume increases. In addition, on sintering

TABLE 1. Physical-Chemical and Thermo-Mechanical Properties of the Experimental Articles

Properties	Borcast-50 W actual data/TU 14-194-271-05	ShSU-33 actual data/GOST 7151-74	ShSU-40 actual data/GOST 7151-74
Mass fraction, %:			
Al_2O_3	55.46/≥ 50	41.25/≥ 33	44.46/≥ 40
Fe_2O_3	1.64	1.51/≤ 1.8	1.42/≤ 1.5
CaO	1.45/(1–2)	—	—
Ultimate compression strength, N/mm ²	73.7/≥ 45	49.3/≥ 25	62.5/≥ 50
Open porosity, %	19.9	15.3/≥ 18	14.7/≥ 18
Apparent density, g/cm ³	2.4/≥ 2.25	2.25	2.3/≥ 2.20
Softening temperature, °C	1420	1440	1460/≥ 1450

Note. The GOST and TU norms are presented after the slash.

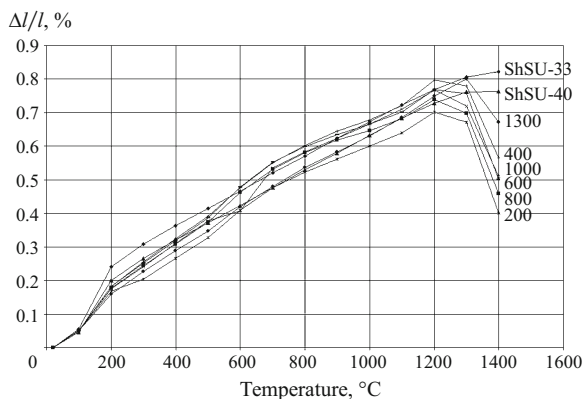


Fig. 2. Relative linear elongation of materials versus temperature (the numbers show the heat-treatment temperature of Borcast-50 W LCRC).

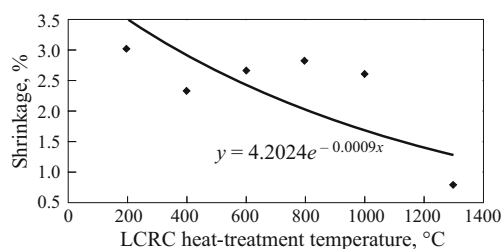


Fig. 3. Shrinkage of LCRC at temperature from 1200 to 1400 °C versus the heat-treatment temperature.

the material also becomes denser, open porosity decreases, and the particles increase in size, which increases the thermal conductivity. The thermal conductivity of Borcast-50 W LCRC changes from 1.30 to 1.52 W/(m · K).

Linear Thermal Expansion. The measurements of the linear thermal expansion of the experimental materials are presented in Fig. 2. Linear expansion is observed for all materials up to temperature 1200 °C. The greatest expansion at 1200 °C was recorded for Borcast-50 W LCRC heat-treated at 400 °C — 0.798% and the lowest value was recorded for the same concrete heat-treated at 200 °C — 0.701%. The relative elongation of calcined ShCU-33 and ShCU-40 articles was 0.769 and 0.729%, respectively.

At temperature above 1200 °C LCRC heat-treatment engendered shrinkage irrespective of the heat-treatment temperature. In addition, the higher the heat-treatment temperature of concrete, the smaller the shrinkage obtained (Fig. 3). The shrinkage must be attributed to sintering processes occurring in LCRC articles.

Given the difference of the thermal expansion of concretes and calcined fireclay articles and the shrinkage of LCRC articles at temperatures above 1200 °C the linear thermal expansion coefficient (CLTE) of the articles was calculated for the temperature interval 20 – 1200 °C (Fig. 4). The largest CLTE was observed for calcined ShSU-33 and ShSU-40 fireclay articles. It was determined that the CLTE

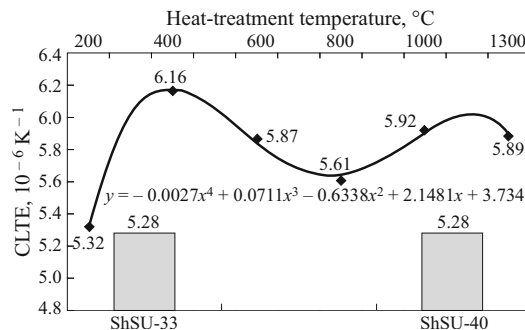


Fig. 4. CLTE of calcined fireclay articles and LCRC articles.

of concrete articles is larger than that of calcined fireclay articles and depends on the temperature of its preliminary heat-treatment. The CLTE is observed to increase at temperatures from 200 to 400 °C, decrease in the interval from 400 to 800 °C (the minimum lies at 800 °C), and then increase once again as the heat-treatment temperature increases.

The changes observed in the CLTE and shrinkage for LCRC articles with increasing heat-treatment are due to changes of the phase composition of the material and the sintering process, which are described in the **Thermal Conductivity** section.

Conclusions from Thermal Conductivity and CLTE Measurements. The calcined ShSU-33 and -40 fireclay articles, which have a stable phase composition formed during calcination, showed the predicted properties:

- thermal conductivity increasing linearly with temperature within small ranges (from 1.43 to 1.47 W/(m · K) for ShSU-33 and from 1.45 to 1.50 W/(m · K) for ShSU-40);
- constant CLTE at temperatures from 20 to 1200 °C.

The Borcast-50 W LCRC properties depend on the heat-treatment temperature. This is due to the changes in the phase composition of the material and the sintering of the concrete matrix.

During service concrete material that is non-calcined or heat-treated at temperature to 1000 °C will heat through and its phase composition will change, which will increase the nonuniformity of heating because of the nonlinearity of the changes in the thermal conductivity. Nonuniform heat-through will cause nonuniform dimensional changes in each isothermal layer. As a result, shear stresses will arise in the material between the layers; these stresses will engender cracking when the ultimate stress is exceeded. The most dangerous situation is the presence of shrinkage in the concrete at temperatures above 1200 °C. The shrinkage causes cracking of the joints between blocks, destroys the integrity of the upper-lying bakor lining of the melting tank in the furnace, and causes leakage of molten glass. A loss of continuity or destruction of even a part of the bottom structure of a glass-making furnace will cause emergency shutdown of the furnace and make it necessary to perform an overhaul with complete disassembly of the entire structure of the glass-making furnace.

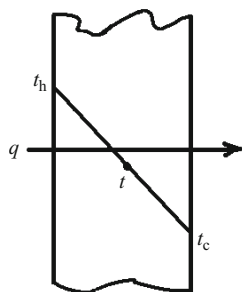


Fig. 5. Diagram of the temperature distribution in a flat uniform wall.

Thermal Stresses. We shall now consider a flat uniform wall in which the heat flux q is directed from the “hot” side with temperature t_h to the “cold” side with temperature t_c (Fig. 5). It is well known that all solids expand when heated. As result of the temperature difference due to the thermal resistance of the material between the layers heated to different temperatures, thermal shear stresses whose magnitude depends on the properties of the material itself (Timoshenko relation) arise [11]:

$$\sigma_t = \frac{\alpha_t E}{1-\mu} (t - t_c),$$

where σ_t is the thermal stress arising between the layers of wall material heated to temperatures t and t_c (temperature of the “cold” side); α_t is the linear thermal expansion coefficient of the wall material at temperature t ; E is Young’s modulus (elastic modulus) of the wall material; and, μ is the Poisson ratio of the wall material.

In refractory masonry at the bottom of a glassmaking furnace articles are positioned in pairs on two sides — along the length and width of the articles. For this reason, thermal bending stresses will arise when a temperature difference is present.

The temperature distribution over the bottom masonry thickness was calculated using the Fourier equation for a flat wall [12]

$$q = -\lambda \frac{dt}{dx},$$

whose solution describes the distribution of the temperature t over the thickness x of the wall (x varies from 0 to S) in the form of a linear function

$$t = -\frac{q}{\lambda} x.$$

The heat flux through the furnace bottom was calculated taking account of the data on the temperature differential along its thickness [12]

$$q = \frac{t_h - t_c}{s/\lambda},$$

where q is the amount of heat passing through unit surface area of the wall, W/m^2 ; t_h is the temperature of the “hot” side

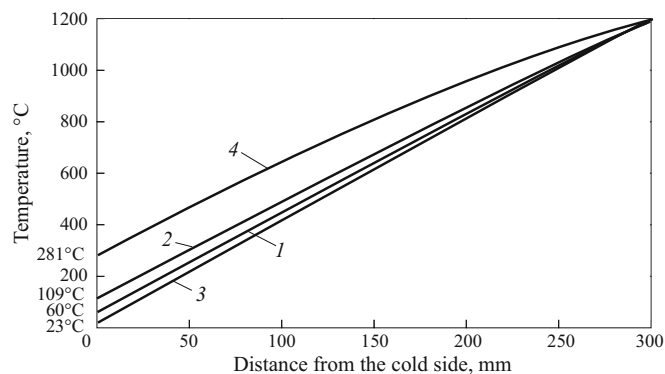


Fig. 6. Temperature distribution along the thickness of the bottom masonry, made of different materials, in a glassmaking furnace: 1) ShSU-33; 2) ShSU-40; 3) Borcast-50 W LCRC heat-treated at 400°C; 4) Borcast-50 W LCRC calcined at 1300°C.

of the wall (1200°C); t_c is the temperature of the “cold” side of the wall (20°C); S is the thickness of the wall (0.3 m); and, λ is the thermal conductivity of the wall material, $W/(m \cdot K)$.

For prescribed values of the parameters the computed heat flux was $5500 W/m^2$. The temperature distribution over the thickness of masonry, made of different materials, at the bottom of a glassmaking furnace is shown in Fig. 6. The data obtained by means of calculations agree with the published data [13]. It is interesting that when articles made of Borcast-50 W LCRC calcined at 1300°C are used the temperature of the “cold” side will be 281°C, and this will require additional heat protection for metal structures touching the refractory articles.

The thermal stresses were calculated using measurements of the thermal conductivity and CLTE for calcined ShSU-33 and -40 fireclay articles as well as Borcast-50 W LCRC concrete articles heat-treated at temperatures 400 and 1300°C. Young’s modulus at room temperature was also determined for these materials (Table 2).

Since the articles in the bottom masonry are squeezed from the sides by neighboring articles and at the edges by the metal barriers of the furnace’s bandage, compression stresses develop in them during thermal expansion. The calculations show (see plots in Fig. 7) that for 1000 – 1100°C temperature differentials thermal stresses appear in all articles irrespective of the their nature. These stresses exceed the ultimate compression strength of the articles: ShSU-33 — by a factor

TABLE 2. Results of the Determination of Young’s Modulus at Room Temperature

Material	Young’s modulus, MPa
Calcined ShSU-33 fireclay articles	12,300
Calcined ShSU-40 fireclay articles	15,590
Borcast-50 W LCRC articles heat-treated at 400°C	18,410
Borcast-50 W LCRC articles heat-treated at 1300°C	25,570

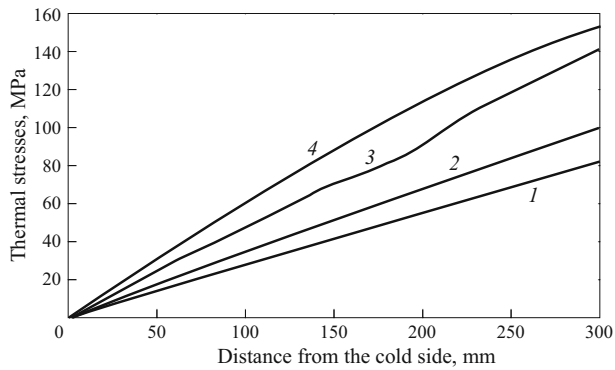


Fig. 7. Computed thermal stresses appearing in refractory bottom masonry of a glassmaking furnace for different materials: 1) ShSU-33; 2) ShSU-40; 3) Borcast-50 W LCRC heat-treated at 400°C; 4) Borcast-50 W LCRC calcined at 1300°C.

of 1.66; ShSU-40 — by a factor of 1.59; Borcast-50 W concrete heat-treated at 1300°C — by a factor 1.40, Borcast-50 W concrete heat-treated at 400°C — by a factor of 1.90. The calculations are in good agreement with the published values [11].

Expansion joints are provided to prevent masonry failure. The use of multilayer lining at the furnace bottom and heat-insulation articles in the outer layer decreases the temperature differentials and thermal stresses.

Conclusions from Thermal Stress Calculations. For single-layer heat insulation of the furnace bottom by 300 mm thick blocks set 160 – 190 mm from the “cold” side thermal stresses exceeding the ultimate compression strength of refractory material arise irrespective of the type of material used. Calcined materials withstand thermal stresses better than non-calcined materials.

Because calcined articles made of LCRC have a high thermal conductivity additional heat protection of the metal structures touching the refractory articles will be necessary if such materials are to be used, since the temperature of the “cold” side will exceed 200°C.

Glass Attack Resistance. Transverse cuts were made to study the interaction of the crucible samples with sheet-glass and container-glass melts. A JEOL-6380LV scanning electron microscope and an INCA energy dispersive spectrometer were used to map the structure of the samples from the glass – refractory contact zone into the interior of the sample. Processing and analysis of the images were performed in the INCA Mapping program. The photographs of the microstructure and the maps obtained for the distribution of the main elements over each zone are presented in Figs. 8 – 11.

After interacting with glass melts all refractory materials acquired zonal structure: contact, transition, and unchanged zones. But the character of the interaction and the width of

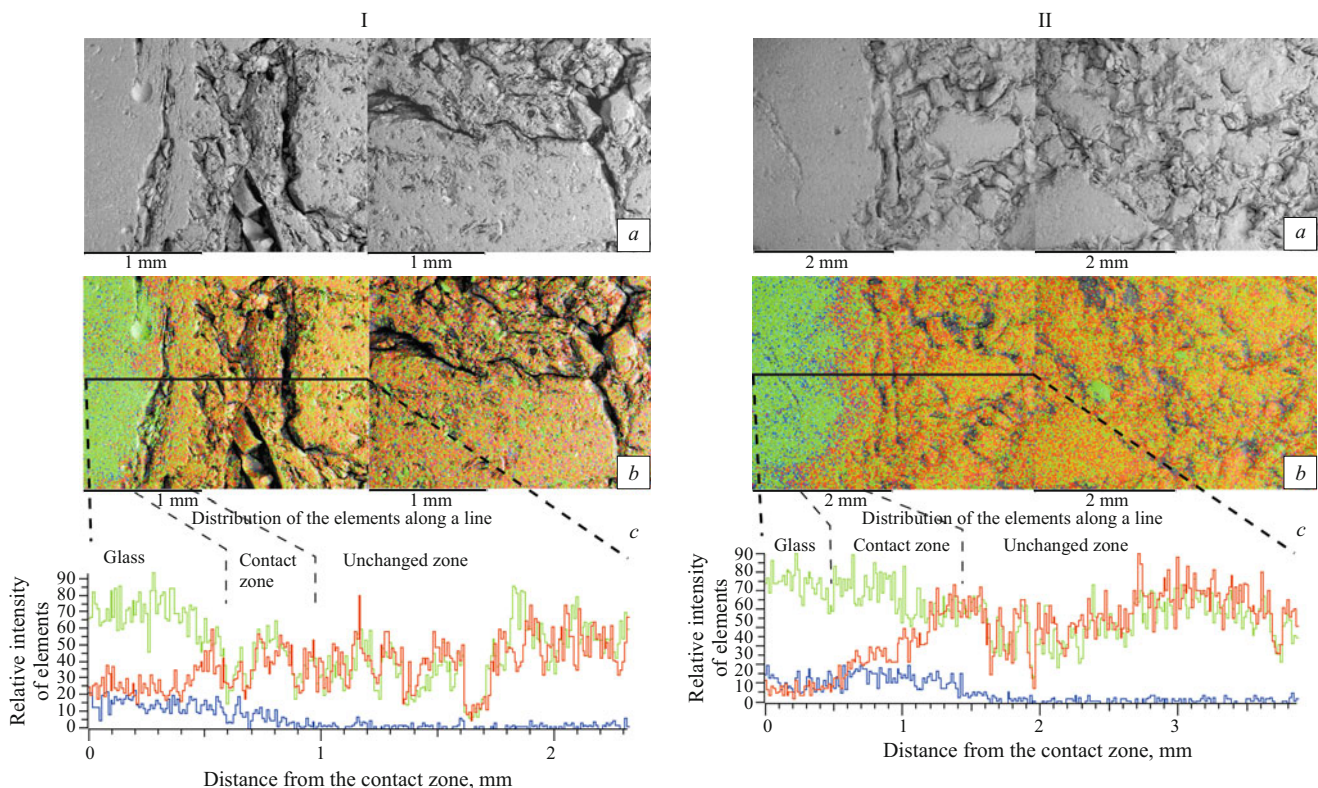


Fig. 8. Tests for glass attack resistance of ShSU-33 parts under the action of sheet (I) and container (II) glass: *a*) photomicrograph of the post-test (1400°C, 5 h) structure of a refractory; *b*) map of the distribution of elements over the zones of a refractory after tests for glass attack resistance [green color) silicon; red) aluminum; blue) potassium]; *c*) plot of the distribution of the elements along a line into the interior of a refractory from the glass – refractory contact zone.

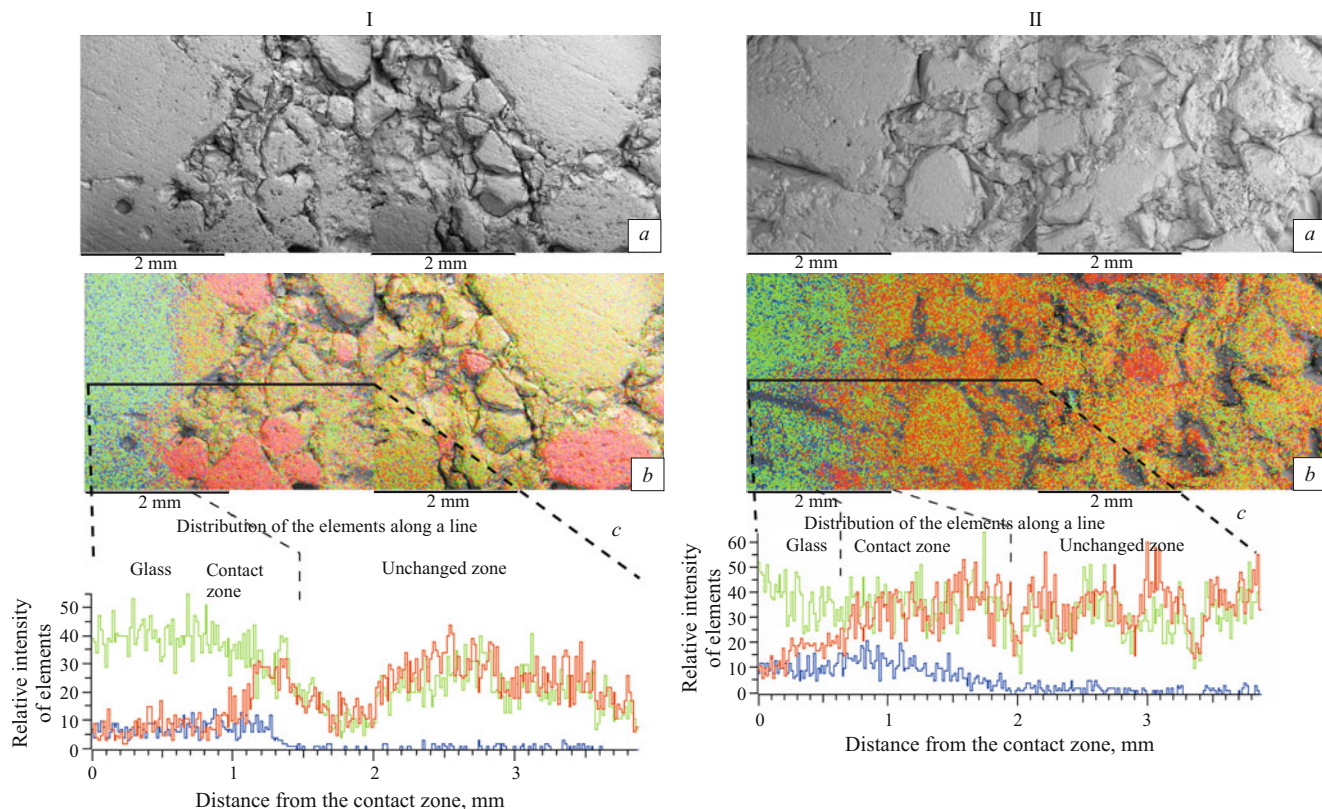


Fig. 9. Tests for glass attack resistance of ShSU-40 parts under the action of sheet (I) and container (II) glass: *a*) photomicrograph of the post-test (1400°C, 5 h) structure of a refractory; *b*) map of the distribution of elements over the zones of a refractory after tests for glass attack resistance [green color) silicon; red) aluminum; blue) potassium]; *c*) plot of the distribution of the elements along a line into the interior of a refractory from the glass – refractory contact zone.

each zone for each of the two groups of materials (calcined fireclay articles and LCRC articles) differ considerably.

For calcined ShSU-33 and -40 fireclay articles, as a result of the action of sheet- and container-glass melt on the

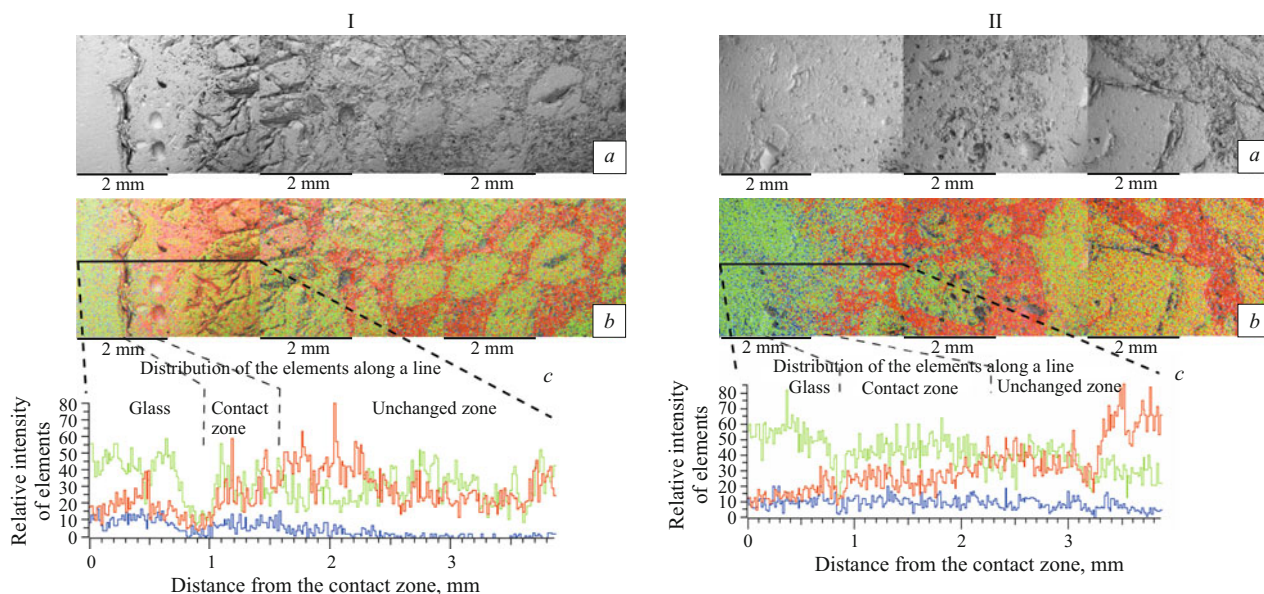


Fig. 10. Tests for glass attack resistance of LCRC Borcast-50 W articles heat-treated at 400°C under the action of sheet (I) and container (II) glass: *a*) photomicrograph of the post-test (1400°C, 5 h) structure of a refractory; *b*) map of the distribution of elements over the zones of a refractory after tests for glass attack resistance [green color) silicon; red) aluminum; blue) potassium]; *c*) plot of the distribution of the elements along a line into the interior of a refractory from the glass – refractory contact zone.

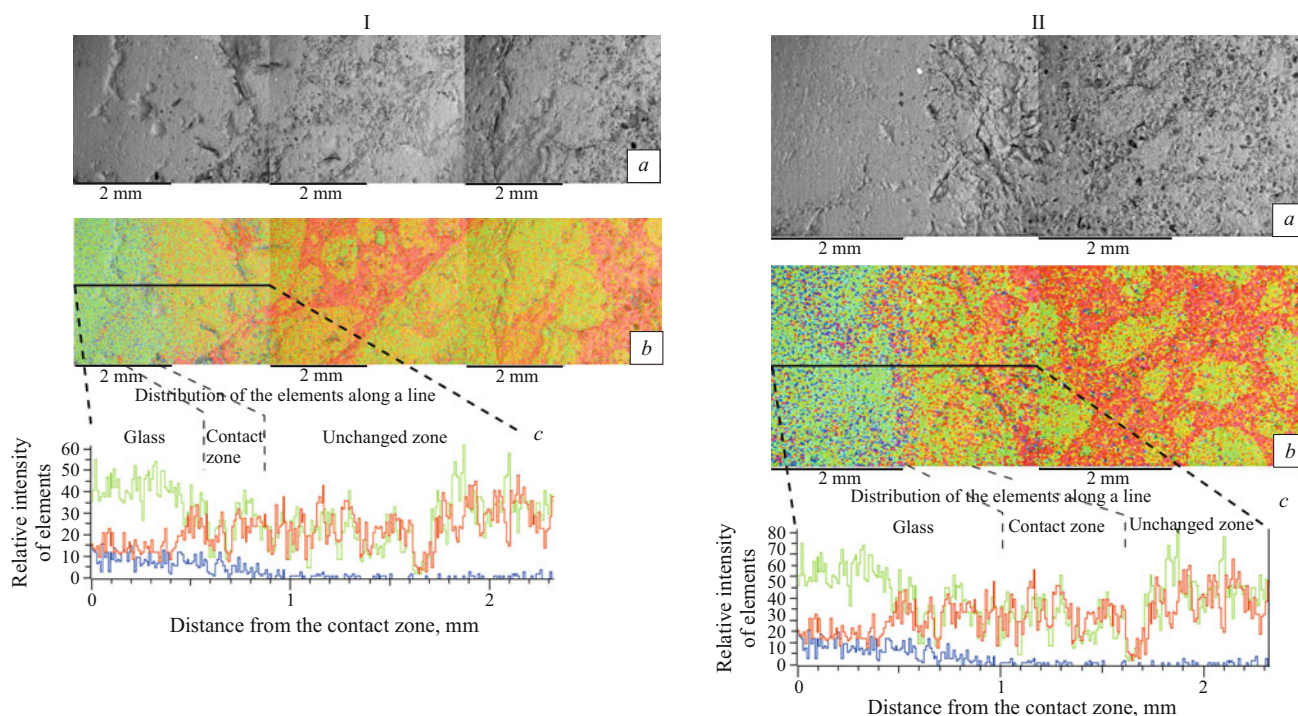
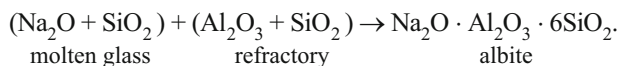


Fig. 11. Tests for glass attack resistance of LCRC Borcast-50 W articles heat-treated at 1300°C under the action of sheet (I) and container (II) glass: *a*) photomicrograph of the post-test (1400°C, 5 h) structure of a refractory; *b*) map of the distribution of elements over the zones of a refractory after tests for glass attack resistance [green color) silicon; red) aluminum; blue) potassium]; *c*) plot of the distribution of the elements along a line into the interior of a refractory from the glass – refractory contact zone.

crucible material a thin 50 – 70 µm wide glass contact layer formed at the glass – refractory boundary in both cases and prevented further permeation and corrosion of the refractory. Mapping the experimental zone confirmed the visual examination of a section of the samples. For container glass, the boundaries of the contact are somewhat smeared, indicating more intense action of the melt as a result of its lower viscosity. In both cases, negligible dissolution of the binder and grain boundaries of the fireclay is observed in the contact layer zone. In subsequent maps the sample appears unchanged. Plots of the change in the intensities of the main elements — Na, Al, and Si — are constructed along the scanning line and confirm the visually established mechanism of the interaction of the refractory with the glass melt. The chemical reactions of the interaction of the aluminosilicate refractory and the molten glass can be schematically described by the equation

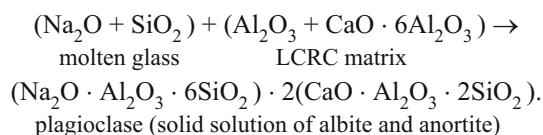


Albite tends to form a high-viscosity glass, which “heals” pores and thereby lowers the diffusion rate of alkali oxides into the interior of the refractory and is a corrosion inhibitor.

The external appearance of the transverse sections of the Borcast-50 W samples reveals that the container-glass melt breaks down the refractory material more rapidly. The width

of the contact layer depends on the heat-treatment temperature of LCRC and ranges from 1 – 3 to 5 mm in articles heat-treated at 1300°C. The section shows that small fireclay and binder grains dissolve. During mapping of the fragments of interest it was found that the boundaries of the glassy contact layer are smeared. The permeation of the refractory (matrix) binder is uniform. Subsequently, the structure of the sample remains unchanged. In the case of interaction with the sheet-glass melt the width of the contact layer is negligible — of the order of 1 mm. The interaction mechanism is similar to the reaction with container glass.

As the heat-treatment temperature of the concrete increases, the corrosion rate decreases but corrosion is not inhibited. The chemical reactions involved in the interaction of the LCRC matrix and the molten glass can be described schematically by the equation



The product of interaction — a solid solution of albite and anortite (plagioclase) — crystallizes at temperatures below 1100°C; its melt has a lower viscosity and is incapable of “healing” pores as albite can. As a result, nothing inhibits the corrosion of the refractory material, and the LCRC matrix material is washed into the molten glass.

The lower resistance to the action of the glass melts of LCRC samples as compared with ShSU-33 and -40 articles is due to the present of high-alumina cement (HAC) in the batch as well as the high content of Al_2O_3 in the binder with an appreciable deficit of silica. In the course of the interaction of the glass melt with concrete, the matrix corundum and calcium aluminates from HAC actively react with the glass and dissolve in it, lowering its viscosity, which makes the reaction more intense.

CONCLUSIONS

The use of articles made of LCRC instead of calcined fireclay for the bottom masonry of a glassmaking furnace is unjustifiably risky for two main reasons:

1) because of their unstable phase composition concrete materials do not have constant thermophysical properties, which change with the heat-treatment temperature; linear expansion of these materials also depends on the heat-treatment temperature, and at temperatures below 1200°C shrinkage replaces expansion; all this taken together promotes growth of the thermal stresses and destroys the continuity of the masonry at the base of the furnace and premature removal of the furnace from operation;

2) the resistance of concretes to the action of glass melt, especially container-glass melt, is lower than that of fireclay articles because of the presence of calcium aluminates and fine alumina in the binding part (matrix).

Calcination of LCRC articles performed at the manufacturing plant makes it possible to stabilize the phase composition of the articles and their thermophysical properties but it does not lower their thermal conductivity, prevent shrinkage at temperatures above 1200°C , or increase resistance to glass attack, though it does decrease the magnitude of the shrinkage and the degree of interaction with glass melt.

Calcined fireclay articles have obvious advantages, determining their longer service life, over LCRC articles:

1) the constancy of the thermophysical properties and linear thermal expansion coefficient makes it possible to predict their behavior during operation; they show no volume changes capable of opening the masonry joints;

2) the inhibition of the contact interaction at the glass – refractory boundary as a result of the formation of a dense contact layer makes it possible to withstand the corrosion action of small molten glass flows for a long time.

A glassmaking furnace contains a number of structural elements in which LCRC articles are used without any special risk: burner blocks of the melting furnace, bottom and top structure of the feeders, and drop-forming ceramic — for container-glass furnaces; block articles (bottom block) of the float-tank — for sheet-glass furnaces. Most of these elements, the float-tank being an exception, can be replaced, if necessary, without stopping the furnace.

REFERENCES

1. V. P. Migal', É. Yu. Panfilova, V. N. Ivanov, et al., "Mastering the manufacture of fireclay block articles for glassmaking furnaces," *Novye Ogneupory*, No. 6, 19 – 25 (2008).
2. G. S. Rossikhina, V. V. Podkholyuzin, E. A. Doroganov, and V. A. Doroganov, "Corrosion resistance of refractory articles made of low-cement concretes for glass production," *Steklo Keram.*, No. 11, 24 – 28 (2006); G. S. Rossikhina, V. V. Podkholyuzin, E. A. Doroganov, and V. A. Doroganov, "Corrosion resistance of refractories made from low-cement concretes for glassmaking," *Glass Ceram.*, **63**(11 – 12), 381 – 385 (2006).
3. G. S. Rossikhina, N. N. Shcherbakova, M. P. Shchedrin, et al., "Study of refractory concrete materials with aluminosilicate composition by petrographic methods," *Steklo Keram.*, No. 11, 28 – 31 (2007); G. S. Rossikhina, N. N. Shcherbakov, M. P. Shchedrin, N. V. Tolubaeva, and T. F. Bukina, "Investigation of refractory concrete materials with aluminosilicate composition by petrographic methods," *Glass Ceram.*, **64**(11 – 12), 404 – 407 (2006).
4. G. S. Rossikhina, M. P. Shchedrin, and N. N. Shcherbakov, "Thermophysical properties of refractory composite materials for glass production," *Steklo Keram.*, No. 5, 26 – 28 (2008); G. S. Rossikhina, M. P. Shchedrin, and N. N. Shcherbakov, "Thermophysical characteristics of refractory composite materials for glass production," *Glass Ceram.*, **65**(5 – 6), 162 – 164 (2008).
5. G. S. Rossikhina, I. V. Murzin, and N. N. Shcherbakova, "Production and application of refractory concretes and the practice of their application in glassmaking units," *Steklo Keram.*, No. 9, 32 – 35 (2008); G. S. Rossikhina, I. V. Murzin, and N. N. Shcherbakova, "Production of refractory of concretes and practice in used them in glassmaking aggregates," *Glass Ceram.*, **65**(9 – 10), 324 – 327 (2008).
6. I. V. Egorov, I. V. Galenko, S. A. Agafonov, and M. P. Ivanova, "New refractories for glassmaking," *Ogneup. Tekh. Keram.*, Nos. 11 – 12, 47 – 50 (2008).
7. Yu. E. Pivinskii, "New refractory concretes and binding systems — fundamental direction in the development, production, and application of refractories in the 21st century. Pt. IV. Low-cement concretes and cement-free non-molded refractories," *Ogneup. Tekh. Keram.*, No. 5, 2 – 10 (1998).
8. *Materials Manufactured by the Lafarge Refractories Company (France), 1992, 15 Years of Use of Low-Cement Concretes in Steel Production* [Russian translation], St. Petersburg (1996).
9. G. V. Krikhbaum, V. Gnauk, I. O. Laurikh, et al., "Advanced matrix system, new approach to self-spreading spinel concretes with high content of aluminum oxide and low content of cement and water," in: *39th International Colloquium on Refractories*, Aachen (1996), pp. 211 – 218.
10. V. P. Migal', A. P. Margishvili, V. V. Skurikhin, et al., "Non-molded refractory materials for the metallurgical industry," *Ogneup. Tekh. Keram.*, Nos. 4 – 5, 27 – 34 (2009).
11. K. K. Strelov, *Structure and Properties of Refractories* [in Russian], Metallurgiya, Moscow (1982), p. 94.
12. P. S. Mamykin, P. V. Levchenko, and K. K. Strelov, *Furnaces and Driers for Refractory Plants* [in Russian], Metallurgizdat, Sverdlovsk (1963), pp. 213 – 221.
13. V. Ya. Dzyuzer and V. S. Shvydkii, *Design of Energy-Efficient Glassmaking Furnaces* [in Russian], Teplotekhnika, Moscow (2009), pp. 311 – 313.